This paper describes objective technical results and analysis. Any subjective views or opinions that might be expressed in the paper do not necessarily represent the views of the U.S. Department of Energy or the United States Government.

SAND2021-2492C

Optimizing Power System Stability Margins After Wide-Area Emergencies

Matthew J. Hoffman
Math. Analysis & Decision Sciences
Sandia National Laboratories
Albuquerque, NM, USA
mjhoffm@sandia.gov

April M. Nelson
Math. Analysis & Decision Sciences
Sandia National Laboratories
Albuquerque, NM, USA
azwerne@sandia.gov

Bryan Arguello
Ops. Rsrch. & Computational Analysis
Sandia National Laboratories
Albuquerque, NM, USA
barguel@sandia.gov

Brian J. Pierre
Electric Power Systems Research
Sandia National Laboratories
Albuquerque, NM, USA
bjpierr@sandia.gov

Ross T. Guttromson
Renewable & Distributed Systems Integration
Sandia National Laboratories
Albuquerque, NM, USA
rguttro@sandia.gov

***Abstract*—Severe, wide-area power system emergencies are rare but highly impactful. Such emergencies are likely to move the system well outside normal operating conditions. Appropriate remedial operation plans are unlikely to exist, and visibility into system stability is limited. Inspired by the literature on Transient Stability Constrained Optimal Power Flow and Emergency Control, we propose a stability-incentivized dynamic control optimization formulation. The formulation is designed to safely bring the system to an operating state with better operational and stability margins, reduced transmission line overlimits, and better power quality. Our use case demonstrates proof of concept that coordinated wide-area control has the potential to significantly improve power system state following a severe emergency.**

***Index Terms*—Wide-area emergencies, optimal control, power system dynamics, power system control, power system stability**

I. Introduction

Dynamic system behavior is important in understanding power system performance in major contingencies. Power system dynamics are modeled by differential algebraic equations (DAEs), with differential equations describing the generators' dynamic response to disturbances and algebraic equations describing power balance. Key optimization problems with dynamics include transient stability constrained optimal power flow (TSCOPF) and more recently first-swing-constrained and transient stability-constrained emergency control (FSCEC and TSEC). TSCOPF and related formulations [1]–[6] optimize *pre-contingency* power flow such that transient stability is guaranteed for some set of contingencies. For a given contingency, FSCEC [7] and TSEC [8]–[10] optimize *post-contingency* emergency control variables to guarantee transient stability. For a recent survey of the transient stability-constrained optimization literature see [5], [6].

Sandia National Laboratories is a multimission laboratory managed and operated by National Technology & Engineering Solutions of Sandia, LLC, a wholly owned subsidiary of Honeywell International Inc., for the U.S. Department of Energy's National Nuclear Security Administration under contract DE-NA0003525.

Most literature on dynamics-constrained optimization for power systems addresses stability in single-component contingencies. We are interested in improving system stability and robustness in *wide-area* emergency cases involving disruption of many components across a wide geographical area. While [11] demonstrated solution of optimal control problems for up to 3 component failures, they did not consider massive multi-component emergencies.

The rapidity of individual failures and cascading dynamics in such an emergency makes successful immediate emergency intervention unlikely. Thus, we focus on improving robustness of the grid once the initial cascading dynamics decay to steady state. This state may be very close to instability boundaries, exceed the ratings of certain components (e.g., power ratings for transmission lines), and/or suffer from serious power quality concerns. We therefore optimize *margins* against key limits to provide more safety margin (e.g., during restoration or in case of follow-on contingencies).

Dynamics-constrained optimization problems are categorized into *direct* formulations that explicitly incorporate the time dynamics of the system in the formulation, and *indirect* formulations that instead take advantage of calculus of variations. We use the direct approach, which tends to have better convergence particularly on path-constrained problems [4], [5], [8], [12] and is prevalent among work demonstrating significant scalability (for example see [7], [8], [10]).

The direct approach requires temporal discretization of the DAE. The most common solutions are *simultaneous* discretization (the DAE is explicit in the constraints, which are all discretized and solved simultaneously) or *sequential* discretization (dynamics are an implicit function, typically updated by a simulation). For a discussion of discretization approaches see [4]. We use sequential discretization, for its ability to take advantage of non-closed-form function evaluations, event detection and processing, adaptive time-stepping, and numerical integration error control within the simulation.

Our work differs from literature in these key ways:

- Enacts control actions at post-contingency steady state following a severe multi-contingency disturbance
- Optimizes penalties defined over stability, quality and operational metrics to provide safety margin, rather than optimizing cost subject to stability or operational constraints
- Uses nonlinear penalty functions to incentivize meeting limits and providing additional safety margin
- Utilizes event thresholds to terminate expensive DAE integration early in infeasible cases

II. General Formulation

This section presents a general dynamic optimization formulation for DAE models. Its application to power systems is described in detail in Section III. We pose a class of penalty minimization nonlinear programs (NLPs) with path constraints:

$$\min_{u} \quad \left(\psi(x,u)|_{t_f} + {}^{1}/_{(t_f - t_o)} \int_{t_0}^{t_f} \Psi(x,u)\, dt \right) \tag{1a}$$

$$\text{s.t.} \quad \Gamma \dot{x} = f(x,u), \; x(0) = x_0, \tag{1b}$$

$$Au \le b, \qquad A_e u = b_e, \tag{1c}$$

$$c(x,u) \le 0, \qquad c_e(x,u) = 0, \tag{1d}$$

$$b_l \le u \le b_u \tag{1e}$$

where ψ and Ψ are scalar penalty functions, x is the system state vector, u is the vector of inputs, Γ is the mass matrix, and t_0 is chosen such that the system is at (post-contingency) steady state, i.e., ${}^{d}/_{dt}(x)|_{t_0} = 0$.

For a power system, states x generally include (at a minimum) the rotor angle δ and frequency ω of each generator, and the voltage V and phase angle θ of each bus. The mass matrix Γ takes the form $\left[\begin{smallmatrix} I & 0 \\ 0 & 0 \end{smallmatrix}\right]$ such that δ and ω are defined by differential equations and V and θ must satisfy (algebraic) power balance.

III. Power System Formulation

Common power system dynamic optimization decision variables include generator power output [3], [5], [7], [8], [10], [13]–[15], voltage [5], [13], [14] and/or power draw at loads [7], [8], [10], [14]. As an OPF sets the initial conditions for the dynamic transient stability assessment sub-problem, most dynamic grid optimization literature does not use time-varying control [4]. However, in our problem, as in TSEC, we wish to assess not only whether a new steady state is possible, but if dynamic control can get the system there safely. There are two implications. First, we update decision variables in time via a linear control profile (similar to [13]). Second, our decision variables are not power and voltage as in an OPF, but *control surfaces* associated with power and voltage: namely, power and voltage control set-points at each generator, and load factor at each load. The load factor enables restoration of previously shed load, or shedding of additional load (discouraged by the objective function, but allowed if benefit is sufficient).

A. Constraints

First we describe the power balance and generator/load dynamics comprising the DAE of (1b). Then we describe the bounds of (1e) and nonlinear stability and operational constraints of (1d), respectively.

1) Power Balance: Power balance at the buses can be expressed in matrix-vector form as

$$0 = Ve^{i\theta} \odot \left(YVe^{i\theta}\right)^{*} + S_{gen} - S_{load} \tag{2}$$

where S_{gen_b} and S_{load_b} are the total complex power injection from generators and total complex power draw from loads at bus $b \in \mathcal{B}$. This defines the algebraic portion of (1b), i.e., the portion where the diagonal of the Γ matrix is zero. We use the nominal-π medium-line assumptions [16] for calculating the admittance matrix Y from parameters of lines $\lambda \in \Lambda$.

2) Generator Dynamics: For generator dynamics we use the fourth-order flux decay generator model from [17] with an added equation (turbine with no reheating) to model how mechanical torque responds to a change in set-point. At each generator $g \in \mathcal{G}$, with index g suppressed except for V_{b_g}:

$$\begin{aligned} P_e &= \left(E'_q + (X_q - X'_d)I_d\right) I_q \\ \dot{\delta} &= \omega - \omega_{ref} \\ \dot{\omega} &= {}^{1}/_{M}(T_m - P_e - D(\omega - \omega_{ref})) \\ \dot{E}_{fd} &= {}^{1}/_{T_A}(K_A(V_{ref} - V_{b_g}) - E_{fd}) \\ \dot{E}'_q &= {}^{1}/_{T'_{do}}(E_{fd} - (E'_q + (X_d - X'_d)I_d) \\ \dot{T}_M &= {}^{1}/_{T_{ch}}(P_{ref} - T_M) \end{aligned} \tag{3}$$

The stator equations [17] define the power injection from the generators at each generator bus, i.e., S_{gen}.

3) Load Dynamics: Load dynamics are important to system stability and are shown to significantly affect real-world feasibility of transient-stability constrained optimization solutions [18]. For our study we use the exponential recovery dynamic load model of [19], modified to allow for load shed by scaling the nominal load power by a load factor (per [20]). At each load $l \in \mathcal{L}$ (index suppressed except for V_{b_l}):

$$\begin{aligned} \dot{x}_p &= -{}^{x_p}/_{T_p} + P_0\left(({}^{V}/_{V_0})^{\alpha_s} - ({}^{V}/_{V_0})^{\alpha_t}\right) \\ \dot{x}_p &= -{}^{x_q}/_{T_q} + Q_0\left(({}^{V}/_{V_0})^{\beta_s} - ({}^{V}/_{V_0})^{\beta_t}\right) \\ P_L &= k_L\left({}^{x_p}/_{T_p} + P_0\left({}^{V}/_{V_0}\right)^{\alpha_t}\right) \\ Q_L &= k_L\left({}^{x_q}/_{T_q} + Q_0\left({}^{V}/_{V_0}\right)^{\beta_t}\right) \end{aligned} \tag{4}$$

4) Decision Variable Bounds: Upper bounds for P_{ref} are set based on the generator ratings. Upper and lower bounds for k_L are set to allow for full load recovery or full load shed, respectively. V_{ref} is allowed to vary by 10% of nominal.

5) Stability and Operational Constraints: Transient stability is approximately modeled by the deviation of the rotor angle from the inertia-weighted average of all generators.

$$\bar{\delta}_g = \left| \delta_g - \frac{\sum_k H_k \delta_k}{\sum_k H_k} \right| \tag{5}$$

Although rotor angle deviation limits are system-dependent and vary across the literature [2], we use the commonly accepted $\pm 100^\circ$ limit. Our constraint is then:

$$\bar{\delta}_g \leq 100^\circ \quad \forall g \in \mathcal{G} \tag{6}$$

This constraint is commonly used in the literature [1], [4], [5], [7]–[11], [21] to model transient stability and "is consistent with industry practice and has been found by utility engineers to be acceptable" [1].

Like much of the literature, we limit voltage and frequency:

$$57 \leq {}^{\omega_g}/_{2\pi} \leq 62 \quad \forall g \in \mathcal{G} \tag{7}$$

$$0.7 \leq V_b \leq 1.2 \quad \forall b \in \mathcal{B} \tag{8}$$

These constraints not only ensure basic power quality, but guard against values that could cause under/over- voltage or frequency tripping. Such values are undesirable both from a modeling perspective, as the model is incapable of tripping and would become invalid, and from a power system operation standpoint, as such tripping could initiate another cascade.

B. Objective Function

We define several metrics below that express the deviation of various quantities from their target values. Each of these metrics, defined per relevant component $i \in \cup\{\mathcal{B}, \mathcal{G}, \mathcal{L}, \Lambda\}$, is then used as an input $z(t)$ into a nonlinear penalty function ϕ, parameterized by a deviation limit ζ:

$$\phi(z_i(t), \zeta) = \left| \frac{z_i(t)}{\zeta} \right|^3 \tag{9}$$

Our polynomial penalty function is similar to that of [3] in which path constraint penalties are exponentiated to ensure smoothness. Our usage of denominator ζ and of a cubic function are designed to provide the following benefits:

1) strongly incentivizes getting the deviation below $|\zeta|$
2) weakly incentivizes providing margin *within* $\pm\zeta$
3) de-emphasizes improvement near the target value.

To illustrate, Figure 1 shows a penalty function ϕ to incentivize voltage within 1 ± 0.05 p.u.

Because of the polynomial penalty growth, metrics farthest outside their limits have highest priority in the minimization. Therefore, relative importance of individual deviation metrics is largely dependent on choice of parameter ζ.

With per-component deviation penalties defined, we then define a global penalty Φ as the norm over all relevant components $i \in \cup\{\mathcal{B}, \mathcal{G}, \mathcal{L}, \Lambda\}$ at a given time.

$$\Phi(z(t), \zeta) = \left(\sum_i \phi\left(z_i(t), \zeta\right)^2 \right)^{1/2} \tag{10}$$

Our penalties Ψ and ψ are:

$$\begin{aligned} \Psi(t) = {} & w_\delta \Phi(\bar{\delta}, 100^\circ) + w_V \Phi(\bar{V}, 0.075 \text{ p.u.}) \\ & + w_\omega \Phi(\bar{\omega}_i, 1 \text{ Hz.}) \\ \psi(t) = {} & w_p \left(\Psi + w_S \Phi(\bar{S}, R) + w_L \Phi(\bar{L}, 1) \right) \end{aligned} \tag{11}$$

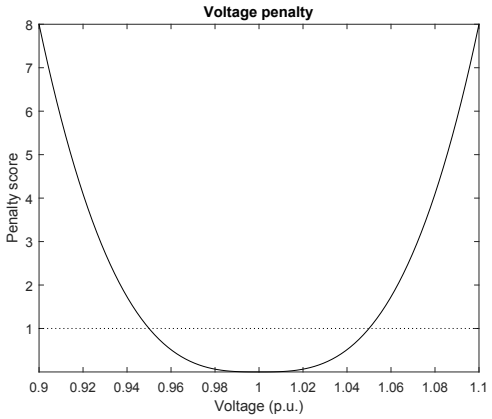

Fig. 1: Voltage penalty $\phi(V, \zeta = 0.05)$ vs. per-unit voltage

In (1a) we minimize the integral of Ψ; this incentivizes quickly reducing its constituent penalty terms (and getting deviations below $|\zeta|$). Terms in ψ are incentivized to reach target values by the end of the time interval. Deviation metrics $\bar{\delta}$, $\bar{V}$, $\bar{\omega}$, $\bar{S}$, and $\bar{L}$ are defined below, subscripted w terms are nonnegative weights, and R gives the short-term line ratings.

1) Transient Stability: Here we reuse $\bar{\delta}_g$ from (5) to measure deviation from center of inertia at each generator g. Penalizing this metric as it approaches 100° incentivizes stability margin so that subsequent dynamics are less likely to cause loss of transient stability.

2) Voltage: It is desirable for voltage to be close to nominal, for power quality reasons and to provide margin against undervoltage and overvoltage tripping (and possibly voltage instability). $\forall b \in \mathcal{B}$:

$$\bar{V}_b = |V_b - 1| \tag{12}$$

3) Line Power Limits: Current flow through lines should be below thermal limits [1], [2], [14], [22]. We represent this via comparison of the power injection into each line against its short-term power rating. For each line $\lambda \in \Lambda$ connecting a pair of buses $j, k \in \mathcal{B}$:

$$\bar{S}_\lambda = max\left(|S_{jk}|, |S_{kj}|\right) \tag{13}$$

where S_{jk} and S_{kj} are the power at the j and k ends of line λ, respectively. Exceeding rating R_λ is disincentivized in (11).

4) Frequency: Similar to voltage, we incentivize near-nominal frequency both for power quality reasons and to provide margin against tripping.

$$\bar{\omega}_g = |\omega_g - \omega_{ref}| \tag{14}$$

5) Load Shed & Restoration: We wish to disincentivize deviation from nominal loading. $\forall l \in \mathcal{L}$:

$$\bar{L}_l = \frac{|P_{Ll} + jQ_{Ll}|}{S_l^{nom}} - 1 \tag{15}$$

Since *any* load shed (including load previously shed in cascading dynamics) will result in a penalty contribution, this provides an opportunistic incentive to *restore* load as well as a penalty for deliberately *shedding* load.

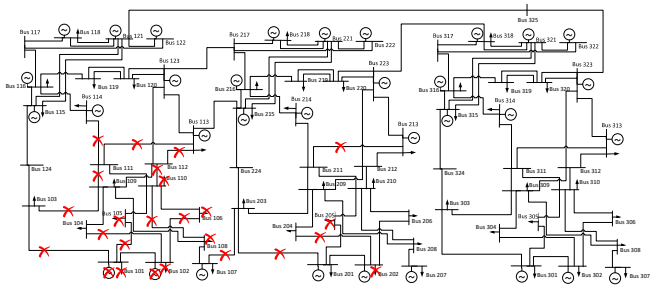

Fig. 2: RTS-96 test system (showing contingency scenario).

IV. Example Implementation

Scenarios are implemented as a series of component trips and subsequent cascading in PSLF [23] on the RTS-96 test system [24], which has 73 buses (51 with loads), 99 machines, and 120 lines. Each PSLF contingency scenario simulation is run to steady state, which becomes the initial condition for a sequential-discretization optimization implemented using the interior point method [25] in Matlab via the function *fmincon*. Initial guesses for generator V_{ref} and P_{ref} set-points and load factor k_L are set to their nominal post-contingency values. Within the inner simulation loop, controls are updated to their new values via a fixed-time linear control profile.

The power system DAE is integrated by *ode15s*, an adaptive-timestep integrator based on the numerical differentiation formulas [26]. Adaptive time-stepping, error control and solution refinement ensure an efficiently and accurately evaluated solution. We use event handling for prompt detection and termination of practically infeasible dynamics in the DAE integration, in which case the interior point method is prompted to backtrack. For event thresholds we use versions of constraints (6)–(8) with relaxed limits.

The high dimensionality (two variables per generator and one per load) makes this problem a natural candidate for variable reduction, both for computational performance and implementability of control actions. Variable selection methods have previously been used with good results in dynamic optimization problems [10], [12]. In this implementation, variable selection is performed using a scaled gradient method. While we are focused on proof-of-concept of a new formulation and not scalability *per se*, we make use of parallel resources for numerical gradient estimation.

A. Results

In one scenario, a sequence of relay failures led to a cascade of events in PSLF, resulting in 15 tripped lines, 8 tripped generators at 2 buses, and 8 tripped loads, with a system-wide load shed of 965 MVA. This scenario is depicted in Figure 2. We analyze the remaining operational component of the network, which has multiple over- and under-voltage issues and one line exceeding its short term power limit. Here, 96 variables (of 249) are included in the optimization, chosen as a compromise between reducing problem size and demonstrating the efficacy of wide-area coordinated control.

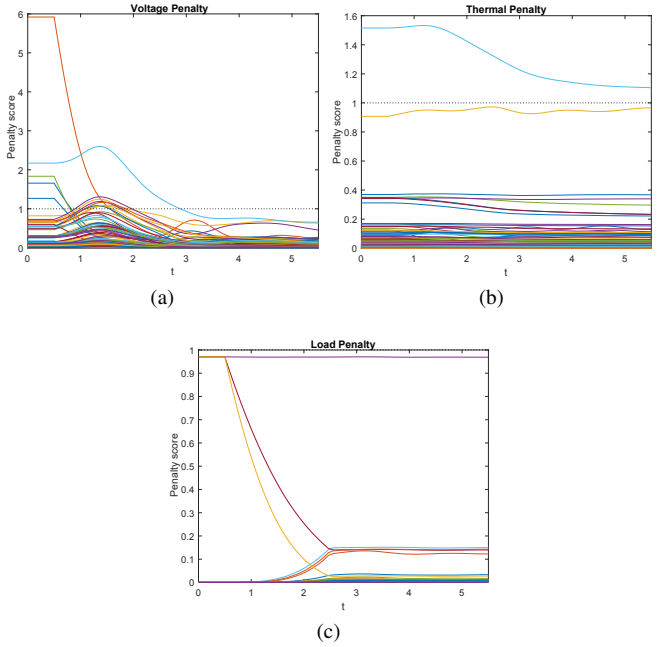

Fig. 3: Trajectory in the optimal solution of (a) voltage penalties at each bus, (b) thermal penalties at each line and (c) load shed penalties at each load.

In Figure 3 we show the trajectories of key penalty measures – i.e., the ϕ functions of the voltage, thermal and load shed deviation metrics of (12), (13) and (15). We can see in 3a that voltage deviations are significantly improved, in 3b the excess line power is reduced, and in 3c that some additional loads are shed (increasing penalties) while others are restored (decreasing penalties). Other penalties (transient stability, frequency deviation) were kept well below 1.0 in this example, indicating near-target values. In Figure 4, note that voltages are quickly brought to more desirable levels (as implied by Figure 3a) while frequency oscillates within acceptable margins before approaching the desired 60 Hz.

Results shown here are representative of several scenarios investigated, which were of similar severity and demonstrated similar significant improvement in several metrics (with others kept within acceptable limits). Most improvement generally occurred within 10 interior point iterations.

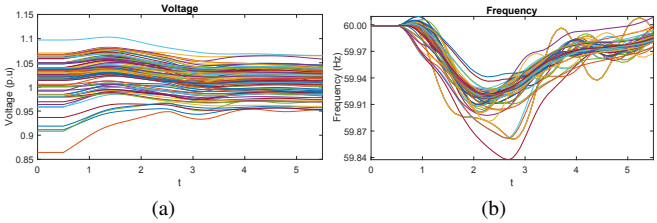

Fig. 4: Trajectory in the optimal solution of (a) voltage at each bus and (b) frequency at each generator.

V. Conclusion

We have described a dynamics-constrained nonlinear programming formulation for optimizing stability margins, operational margins and power quality following a wide-area power system disturbance, via generator control, load shedding and load restoration. Solution of this problem provides improved margin for error during recovery and restoration, as well as safety margin should any additional contingencies occur, and poses a significantly improved starting point for recovery operations.

We have demonstrated such coordinated wide-area control on severe contingency scenarios on the RTS-96 test system. Novel aspects of this work include: a focus on severe multi-contingency disturbances, nonlinear objective penalties devised to incentivize the most important quality and operational improvements first, and use of event detection to terminate DAE integration of infeasible cases.

This problem presents several interesting opportunities for future work. The sequential discretization framework could allow consideration of other important stability or operational metrics that cannot be expressed in closed form. Examples include small signal stability [14] (calculated based on eigenvalues of the linearized differential system), the canonical Equal Area Criterion (EAC) transient stability calculation [16], and voltage stability metrics such as the Voltage Collapse Proximity Index (VCPI) [15]. Additional controls could be considered, e.g., controllable transformer ratios [13], shunt reactances [13], and control of energy storage [21]. Topology switching [22] may be valuable for certain contingencies, and imposing discrete load shed levels (like [9]) would improve realism; addressing the computational and scalability challenges posed by addition of such discrete decisions warrants further research.

References

[1] D. Gan, R. J. Thomas, and R. D. Zimmerman, "Stability-constrained optimal power flow," *IEEE Transactions on Power Systems*, vol. 15, no. 2, pp. 535–540, 2000.

[2] R. Zárate-Miñano, T. Van Cutsem, F. Milano, and A. J. Conejo, "Securing transient stability using time-domain simulations within an optimal power flow," *IEEE Transactions on Power Systems*, vol. 25, no. 1, pp. 243–253, 2009.

[3] S. Abhyankar, V. Rao, and M. Anitescu, "Dynamic security constrained optimal power flow using finite difference sensitivities," in *2014 IEEE PES General Meeting Conference & Exposition*. IEEE, 2014, pp. 1–5.

[4] G. Geng, V. Ajjarapu, and Q. Jiang, "A hybrid dynamic optimization approach for stability constrained optimal power flow," *IEEE Transactions on Power Systems*, vol. 29, no. 5, pp. 2138–2149, 2014.

[5] S. Abhyankar, G. Geng, M. Anitescu, X. Wang, and V. Dinavahi, "Solution techniques for transient stability-constrained optimal power flow–Part I," *IET Generation, Transmission & Distribution*, vol. 11, no. 12, pp. 3177–3185, 2017.

[6] G. Geng, S. Abhyankar, X. Wang, and V. Dinavahi, "Solution techniques for transient stability-constrained optimal power flow–Part II," *IET Generation, Transmission & Distribution*, vol. 11, no. 12, pp. 3186–3193, 2017.

[7] Q. Jiang, Y. Wang, and G. Geng, "A parallel reduced-space interior point method with orthogonal collocation for first-swing stability constrained emergency control," *IEEE Transactions on Power Systems*, vol. 29, no. 1, pp. 84–92, 2013.

[8] Z. Li, G. Yao, G. Geng, and Q. Jiang, "An efficient optimal control method for open-loop transient stability emergency control," *IEEE Transactions on Power Systems*, vol. 32, no. 4, pp. 2704–2713, 2016.

[9] Z. Li, G. Geng, and Q. Jiang, "Transient stability emergency control using asynchronous parallel mixed-integer pattern search," *IEEE Transactions on Smart Grid*, vol. 9, no. 4, pp. 2976–2985, 2016.

[10] G. Gan, Z. Zhu, G. Geng, and Q. Jiang, "An efficient parallel sequential approach for transient stability emergency control of large-scale power system," *IEEE Transactions on Power Systems*, vol. 33, no. 6, pp. 5854–5864, 2018.

[11] G. C. Zweigle and V. Venkatasubramanian, "Wide-area optimal control of electric power systems with application to transient stability for higher order contingencies," *IEEE Transactions on Power Systems*, vol. 28, no. 3, pp. 2313–2320, 2013.

[12] M. Paramasivam, A. Salloum, V. Ajjarapu, V. Vittal, N. B. Bhatt, and S. Liu, "Dynamic optimization based reactive power planning to mitigate slow voltage recovery and short term voltage instability," *IEEE Transactions on Power Systems*, vol. 28, no. 4, pp. 3865–3873, 2013.

[13] F. Capitanescu, T. Van Cutsem, and L. Wehenkel, "Coupling optimization and dynamic simulation for preventive-corrective control of voltage instability," *IEEE Transactions on Power Systems*, vol. 24, no. 2, pp. 796–805, 2009.

[14] R. Zárate-Miñano, F. Milano, and A. J. Conejo, "An OPF methodology to ensure small-signal stability," *IEEE Transactions on Power Systems*, vol. 26, no. 3, pp. 1050–1061, 2011.

[15] S. S. Asghari, P. Rabbanifar, S. A. Asghari, and D. Azizi, "A multi-objective optimal power flow model for transient and voltage stability improvement," in *2017 IEEE 7th International Conference on Power and Energy Systems (ICPES)*. IEEE, 2017, pp. 80–84.

[16] P. Kundur, N. J. Balu, and M. G. Lauby, *Power system stability and control*. McGraw-Hill New York, 1994, vol. 7.

[17] P. W. Sauer, M. A. Pai, and J. H. Chow, *Power system dynamics and stability: with synchrophasor measurement and power system toolbox*. John Wiley & Sons, 2017.

[18] R. Zhang, Y. Xu, W. Zhang, Z. Y. Dong, and Y. Zheng, "Impact of dynamic load models on transient stability-constrained optimal power flow," in *2016 IEEE PES Asia-Pacific Power and Energy Engineering Conference (APPEEC)*. IEEE, 2016, pp. 18–23.

[19] D. Karlsson and D. J. Hill, "Modelling and identification of nonlinear dynamic loads in power systems," *IEEE Transactions on Power Systems*, vol. 9, no. 1, pp. 157–166, 1994.

[20] S. Arnborg, G. Andersson, D. J. Hill, and I. A. Hiskens, "On influence of load modelling for undervoltage load shedding studies," *IEEE Transactions on Power Systems*, vol. 13, no. 2, pp. 395–400, 1998.

[21] M. Rostami and S. Lotfifard, "Scalable coordinated control of energy storage systems for enhancing power system angle stability," *IEEE Transactions on Sustainable Energy*, vol. 9, no. 2, pp. 763–770, 2017.

[22] P. Dehghanian, Y. Wang, G. Gurrala, E. Moreno-Centeno, and M. Kezunovic, "Flexible implementation of power system corrective topology control," *Electric Power Systems Research*, vol. 128, pp. 79–89, 2015.

[23] GE Energy Consulting, "GE PSLF," https://www.geenergyconsulting.com/practice-area/software-products/pslf, 2020 (accessed August 3).

[24] C. Grigg, P. Wong, P. Albrecht, R. Allan, M. Bhavaraju, R. Billinton, Q. Chen, C. Fong, S. Haddad, S. Kuruganty *et al.*, "The IEEE reliability test system-1996. A report prepared by the reliability test system task force of the application of probability methods subcommittee," *IEEE Transactions on Power Systems*, vol. 14, no. 3, pp. 1010–1020, 1999.

[25] R. H. Byrd, M. E. Hribar, and J. Nocedal, "An interior point algorithm for large-scale nonlinear programming," *SIAM Journal on Optimization*, vol. 9, no. 4, pp. 877–900, 1999.

[26] L. F. Shampine and M. W. Reichelt, "The Matlab ODE suite," *SIAM journal on scientific computing*, vol. 18, no. 1, pp. 1–22, 1997.